

# Comparison of Column-Integrated Aerosol Optical and Physical Properties in an Urban and Suburban Site on the North China Plain

FAN Xuehua<sup>\*1</sup>, XIA Xiang'ao<sup>1,2</sup>, and CHEN Hongbin<sup>1,2</sup>

<sup>1</sup>Key Laboratory of Middle Atmosphere and Global Environment Observation, Institute of Atmospheric Physics, Chinese Academy of Sciences, Beijing 100029

<sup>2</sup>Collaborative Innovation Center on Forecast and Evaluation of Meteorological Disasters, Nanjing University of Information Science & Technology, Nanjing 210044

(Received 16 May 2014; revised 19 July 2014; accepted 12 August 2014)

## ABSTRACT

The column-integrated optical properties of aerosol in Beijing and Xianghe, two AEROSOL ROBOTIC NETWORK (AERONET) sites situated on the North China Plain (NCP), are investigated based on Cimel sunphotometer measurements from October 2004 to June 2012. The outstanding feature found is that the seasonal medians of aerosol optical depth (AOD) at the two stations are in good agreement. The correlation coefficients and the absolute differences between AOD at the two stations are larger than 0.84 and less than 0.05, respectively. Good agreement in AOD at these two sites (one urban and the other suburban; 70 km apart) indicates that aerosol pollution in the Greater Beijing area is regional in nature. However, we find significant differences in the absorption Ångström Exponent (AAE), the real and imaginary part of the refractive index, and thereby the single scattering albedo (SSA), and the difference is seasonally dependent. The feature is found to be more prominent in fall when the fine-mode fraction (FMF) and fine-mode effective radius are significantly different at the two stations, besides the parameters mentioned above. The SSA in Beijing at four wavelengths shows lower values as compared to those in Xianghe, although the difference is not significant in some cases. Significant differences in AAE and fine-mode effective radius indicate that there are differences in aerosol physical and chemical properties in urban and suburban regions on the NCP.

**Key words:** aerosol, optical properties, North China Plain

**Citation:** Fan, X. H., X. A. Xia, and H. B. Chen, 2015: Comparison of column-integrated aerosol optical and physical properties in an urban and suburban site on the North China Plain. *Adv. Atmos. Sci.*, **32**(4), 477–486, doi: 10.1007/s00376-014-4097-0.

## 1. Introduction

Aerosol plays an important role in climate change via its radiative and microphysical effects (Li et al., 2007b). The annual mean of aerosol optical depth (AOD) at 750 nm in China increased from 0.38 in 1960 to 0.47 in 1990 (Qiu and Yang, 2000; Luo et al., 2001), and visibility decreased by 35% from the 1960s to the 1980s (Li et al., 2011). It is widely suggested that the regional climate changes that have occurred over the past half a century in China, such as the weakening of the East Asian monsoon, the cooling in the Yangtze Delta region and Sichuan Basin, as well as the widespread dimming in eastern China, are closely related to an increase of aerosol loading in China (Li et al., 2007b, 2011), although there is still large uncertainty concerning the effects of aerosol on regional climate changes. Because of the large spatiotemporal variation of aerosol properties, further understanding of the effects of

aerosol on climate requires long-term accurate observations of aerosol key properties, especially in heavy polluted regions, e.g., the North China Plain (NCP). The NCP, shown in Fig. 1, is bordered on the north by the Yanshan Mountains, on the west by the Taihang Mountains, and on the south by the Jianghuai Plain (Xia et al., 2013a). From the southeast to the northeast, the plain fronts the Yellow Sea, the Shandong Peninsula, and the Bohai Sea. The NCP is one of the most densely populated regions in China. Unprecedented economic development and population growth on the NCP have taken place over the past three decades, which has resulted in a general decline in air quality (Xia et al., 2007; Li et al., 2011; Xia et al., 2013a). The region is often covered by a thick layer of haze, and the annual mean AOD at 500 nm is 0.82 (Xia et al., 2006; Li et al., 2007c). Aerosol composition and sources over the NCP are very complex, including not only fine aerosol particles from human activities, but also coarse dust particles transported from remote dust regions (Li et al., 2007c; Yu et al., 2007; Li et al., 2013, 2014).

Advances in ground-based observation techniques and

\* Corresponding author: FAN Xuehua  
Email: fxh@mail.iap.ac.cn

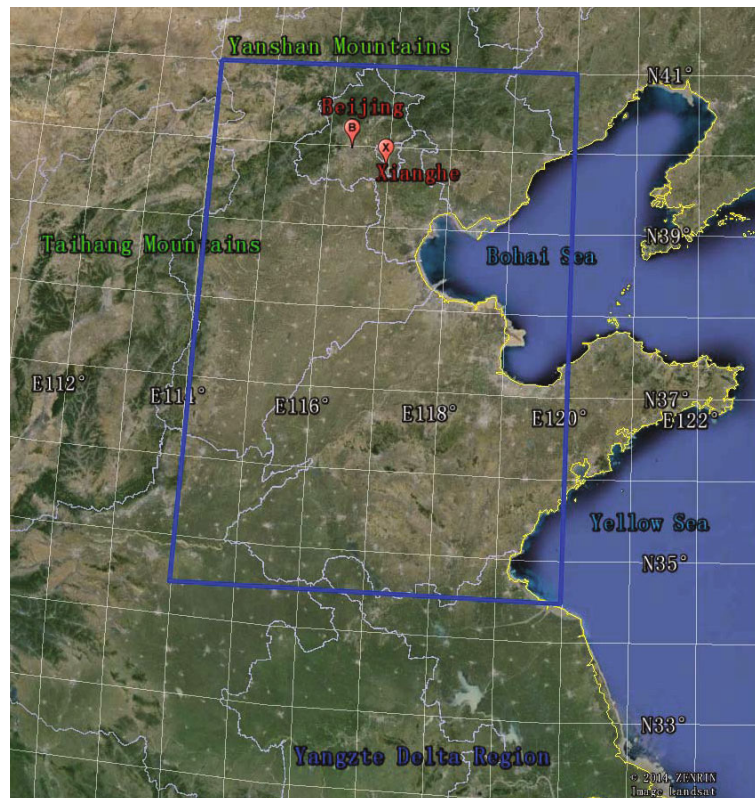


**Fig. 1.** Google Earth map of the NCP ( $34.5^{\circ}$ – $41^{\circ}$ N,  $114^{\circ}$ – $120^{\circ}$ E) and the two AERONET stations [urban Beijing ( $39.98^{\circ}$ N,  $116.38^{\circ}$ E) and suburban Xianghe ( $39.75^{\circ}$ N,  $116.92^{\circ}$ E)].

analysis methods have led to ground-based remote sensing being one of the best-suited methods for deriving reliable and persistent detailed data on aerosol properties in key locations around the world (Xia et al., 2006). The AEROSOL RObotic NETwork (AERONET) is a well-known ground-based aerosol-monitoring network that uses the Cimel CE-318 sunphotometer as its standard instrument. High-quality and detailed analyses of aerosol optical properties from more than 450 AERONET sites have yielded a complete characterization of aerosol optical properties for a wide range of applications (Holben et al., 2001; Che et al., 2009; Eck et al., 2010). In order to investigate the long-term changes in atmospheric aerosol and their spatial variation at a regional scale, two AERONET sites were established on the NCP in April 2002 (Beijing) and in October 2004 (Xianghe). Analysis of data from these AERONET sites has shown a distinct seasonal and interannual variation of aerosol optical properties (Xia et al., 2007) and the climatological aspects of the optical properties of fine/coarse mode aerosol mixtures (Eck et al., 2010; Xia et al., 2013a). High aerosol loading and strong absorption have been shown to reduce daily mean surface solar radiation by  $\sim 30$ – $40 \text{ W m}^{-2}$  (Li et al., 2007c; Xia et al., 2007). The AERONET data have also been used to validate satellite retrievals (Mi et al., 2007; Fan et al., 2008, 2009; Guo et al., 2009) and ground-based lidar retrievals (Nishizawa et al., 2010). Analysis of AERONET data in spring 2001 showed that the AOD and Ångström ex-

ponent in Beijing were very close to those in Xianghe (Eck et al., 2005; Xia et al., 2005), indicating that aerosol pollution over the NCP is regional in nature. The objective of this paper is to extend this analysis to other seasons and to investigate the potential spatial variation of more important aerosol optical and physical properties based on AERONET data at these two sites. The paper is structured as follows: The sites, data and methodology are introduced in section 2. Section 3 presents the time series of the monthly means of the main parameters, including AOD at 675 nm, water vapor content (WV), Ångström exponent (AE) at 440–870 nm, single scattering albedo (SSA) at 675 nm, absorption Ångström exponent (AAE) at 440–870 nm, and fine mode fraction (FMF) at 675 nm at the Beijing and Xianghe sites. The seasonal variation of aerosol optical properties at Beijing and Xianghe, as well as a detailed comparison of aerosol properties at the two sites, are given in section 4. And finally, a discussion and conclusions are presented in section 5.

## 2. Sites, data and methodology

### 2.1. Sites

Beijing ( $39.98^{\circ}$ N,  $116.38^{\circ}$ E), the capital of China, is a megacity with a population of over 20 million people. Beijing is surrounded by the Yanshan Mountains from the west

to the northeast and has heavily industrialized areas from the southwest to the east (Garland et al., 2009). The total vehicle population in Beijing increased to more than 5 million vehicles by the end of 2012. In recent years, automobile exhaust fumes in urban areas have been important contributors to air pollution in Beijing (Hao and Wang, 2005).

Xianghe (39.75°N, 116.96°E), with a population of 310 000, a county of Hebei Province, is located between the two megacities of Beijing and Tianjin. The site is surrounded by cropland, densely occupied residences and light industry. The demand for heating and associated combustion activities increases in winter, when coal-fueled boilers and coal-burning stoves are used for households (Li et al., 2007a).

During the spring season, strong winds occasionally transport desert dust from Northwest China to Beijing and Xianghe, which substantially affects aerosol properties and results in regional air pollution (Eck et al., 2005; Xia et al., 2005). During the summer season, southeasterly winds are dominant and aerosol properties at these two sites are likely affected by anthropogenic aerosols in southern regions. There are two crop residue burning seasons on the NCP: wheat straw and maize stalks are burned in fields in June and October, respectively (Xia et al., 2013b). In addition, Beijing and Xianghe are not only impacted by local pollution, but also by pollution from surrounding areas. For example, it was reported that regional sources could be crucial contributors to aerosol pollution in Beijing (Zhang et al., 2013). The neighboring provinces of Hebei, Shandong and Tianjin Municipality all exert significant influence on air quality in Beijing, partly as a consequence of the prevailing south/southeasterly flow during the summer and the mountains to the north and northwest.

## 2.2. AERONET data

Direct and diffuse spectral radiances are measured by the Cimel CE318 sunphotometer, which are used to retrieve aerosol physical and optical properties such as size distribution, single scattering albedo etc. based on the algorithm of Dubovik and King (2000) and Dubovik et al. (2006). Version 2 and level 2 AERONET data from October 2004 to June 2012 are used in this paper (<http://aeronet.gsfc.nasa.gov/>). Further details on the version 2 algorithm can be found in the works of Dubovik et al. (2006) and Eck et al. (2008).

Aerosol optical and physical properties in the AERONET database include AOD, AE, refractive index, size distribution, SSA, absorption AOD, and asymmetry factor. Furthermore, some other important parameters can be derived from these basic retrievals. For example, the AAE (defined as the negative of the slope of a log-log plot of the aerosol absorption optical depth versus wavelength) provides an indication of the dominance of carbonaceous particles or iron oxides in dust (Bergstrom et al., 2007, 2010). The spectral difference of the AE ( $\alpha$ ) wavelength pairs is a good indicator of fine mode effective radius (Gobbi et al., 2007; Xia et al., 2013a). AOD vs.  $\delta\alpha$  vs.  $\alpha_{440-870\text{ nm}}$  space is plotted to be the framework for analyzing aerosol properties, where  $\delta\alpha$  is the AE difference between  $\alpha_{440-675\text{ nm}}$  and  $\alpha_{675-870\text{ nm}}$ . This space

is invariant to changes in AOD for a given size distribution. Any AOD will be at the same point if the fine and coarse modes stay the same. This space is sensitive to the balance between the fine and coarse modes and is therefore ideal to separate processes related to fine-sized aerosol from the extinction fraction (Gobbi et al., 2007). Cloud contamination will enhance the weight of the coarse mode, while hydration will lead to a growth in both the fine-mode size and fine-mode fraction (FMF) of total AOD. All these aerosol properties are used for the comparison.

## 2.3. Wilcoxon rank sum test

The Wilcoxon rank sum test is a nonparametric test of the null hypothesis that two populations are the same against the alternative that they are not the same (Wild and Seber, 1999). The test is performed based on observational samples from each of two populations, i.e., A with  $n_A$  observations and B with  $n_B$  observations, respectively. The rank of  $n_A+n_B$  observations of the combined sample were calculated and thereby each observation has a rank. It is used to test the possibility of these four situations: the distribution of A is the same as that in B, the distribution of A shifted to the right or left of distribution B, and a shift in a particular direction is not expected with strong prior reason. The Wilcoxon test is valid for data from both normal and non-normal distributions. For non-normal distributions, the Wilcoxon test is more efficient than the  $t$ -test (Wild and Seber, 1999).

The two-sided rank sum test of the null hypothesis is applied to the two independent samples (one from Beijing and one from Xianghe) coming from distributions with equal medians, against the alternative that they do not have equal medians.

## 3. Time series of monthly means of the main parameters

Figures 2a–f respectively show the time series of the monthly means of AOD at 675 nm, WV, AE at 440–870 nm, SSA at 675 nm, AAE at 440–870 nm, and FMF at 675 nm for the Beijing and Xianghe sites. AOD values are higher during the summer months at the two sites. Total column-integrated water vapor and surface relative humidity (RH) are maximum in summer. This results in greater aerosol hygroscopic growth and greater optical extinction in summer (Eck et al., 2005). The seasonal variation of SSA is similar to that of AOD, with higher values (generally greater than 0.90) during the summer months.

The AOD shows a weak decrease during the available observation period at the two sites. It is notable that AOD is lower during 2009 than other years. A lower AOD in 2009 is also found at other Chinese AERONET sites: Taihu, SACOL (Semi-Arid Climate environment Observatory of Lanzhou University) and Xinglong (Fan et al., 2013). In addition, the decrease of AOD during 2009 can also be derived from Moderate Resolution Imaging Spectroradiometer (MODIS) AOD



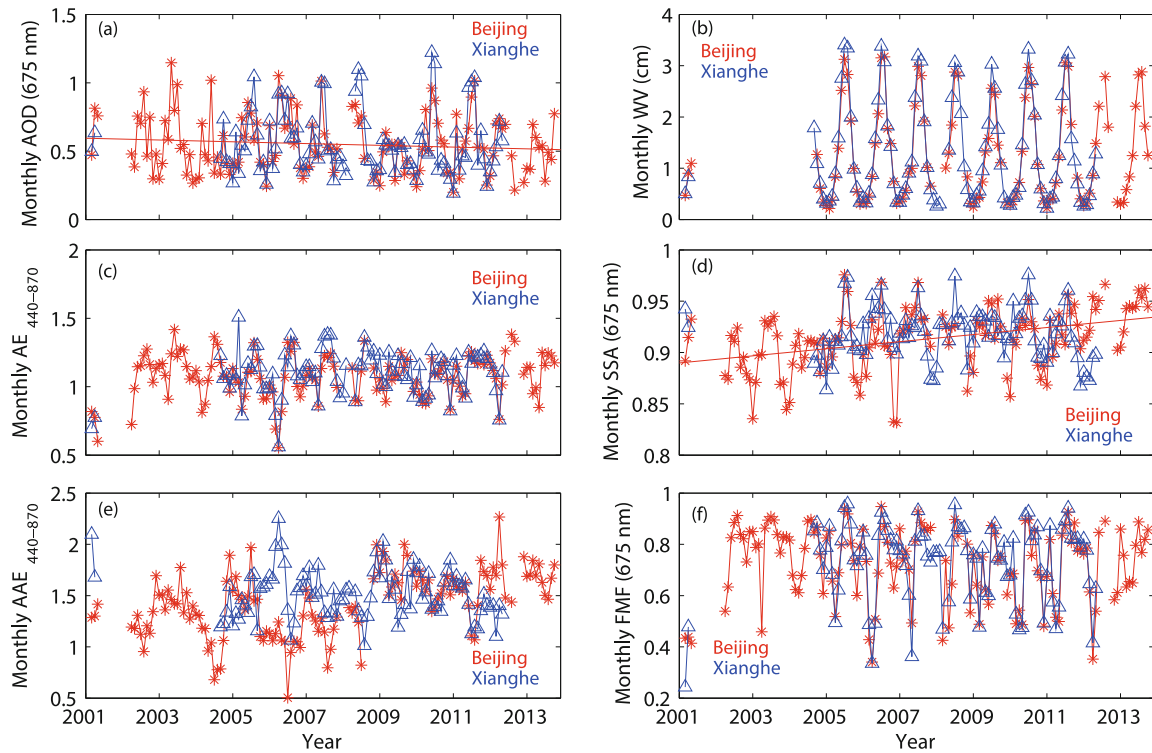


**Fig. 2.** Time series plots of monthly means of (a) aerosol optical depth (AOD) at 675 nm, (b) water vapor (WV) content, (c) Ångström exponent (AE) at 440–870 nm, (d) single scattering albedo (SSA) at 675 nm, (e) absorption Ångström exponent (AAE) at 440–870 nm, and (f) fine-mode fraction (FMF) at 675 nm for the Beijing and Xianghe sites.

time series around the Beijing site (Xia et al., 2013a). The Chinese government took actions to control atmospheric pollution before the Beijing Olympic Games, mainly targeting the heavy pollution factories, transportation and coal-burning activities (Wang et al., 2010). From 20 July to 20 September 2008, Beijing conducted the strict Olympic traffic demand management (TDM) of odd–even day vehicle operation (Wang et al., 2009). The lower AOD from late 2008 that lasted through 2009 is likely associated with pollution control measures taken for the Beijing Olympic Games in 2008 and the economic recession from late 2008 to mid 2009 (Lin et al., 2013).

The SSA at 675 nm is found to increase by  $\sim 0.029$  over 12 years at Beijing, which resembles previous results (Lyapustin et al., 2011). The SSAs at 440, 870 and 1020 nm are also found to increase from 2001 to 2013 at Beijing. The SSA at 675 nm also increases  $\sim 0.021$  from 2001 to 2011 at Xianghe. A possible reason for the reduction of the aerosol absorption is the regulation of black carbon (BC) emissions over Beijing. The Law on the Prevention and Control of Air Pollution was passed in China from 2001 and measurements of improving air quality were enforced further for the 2008 Summer Olympics from 2005. The BC reduced by 31% in Beijing from 2005 to 2008 according to the long term measurements of chemical compositions (Lyapustin et al., 2011). The reduction of total absorption is due to the BC reduction of primary aerosols from local sources (Lyapustin et al., 2011). The variation trends of other parameters are insignificant dur-

ing the available observation period.

#### 4. Comparison of aerosol optical and physical properties at Beijing and Xianghe

The seasonal distribution of AOD at 675 nm, AE ( $\alpha_{440-870 \text{ nm}}$ ), water vapor (WV), and the AE difference between  $\alpha_{440-675 \text{ nm}}$  and  $\alpha_{675-870 \text{ nm}}$  ( $\delta_\alpha$ ) are shown in box-and-whisker plots in Fig. 3. Similarly, Fig. 4 shows the seasonal statistics of FMF at 675 nm, the fine mode effective radius ( $r_f$ ), and AAE (440–870 nm) at Beijing and Xianghe. In the plot, the lower and upper limits of each box represent the 25th and 75th percentiles of the distribution. The central bars and the solid dots in each box are the medians and the geometric means, respectively. The ends of the whiskers indicate the spread of the distribution with the length being 1.5 times the difference between the 75th and 25th percentiles. The values beyond the limits of those lines are drawn as outliers represented by plus signs. The box is shaded if the Wilcoxon rank sum test result is a rejection of the null hypothesis at the 5% significance level. In other words, the median values of aerosol properties at the two sites are significantly different at the 95% confidence level if they are shaded.

The first interesting feature is that there is a distinct seasonal variation of these parameters. Quite similar seasonal variation of AOD, AE and water vapor can be seen, which resembles previous results (Xia et al., 2007; Li et al., 2007c;

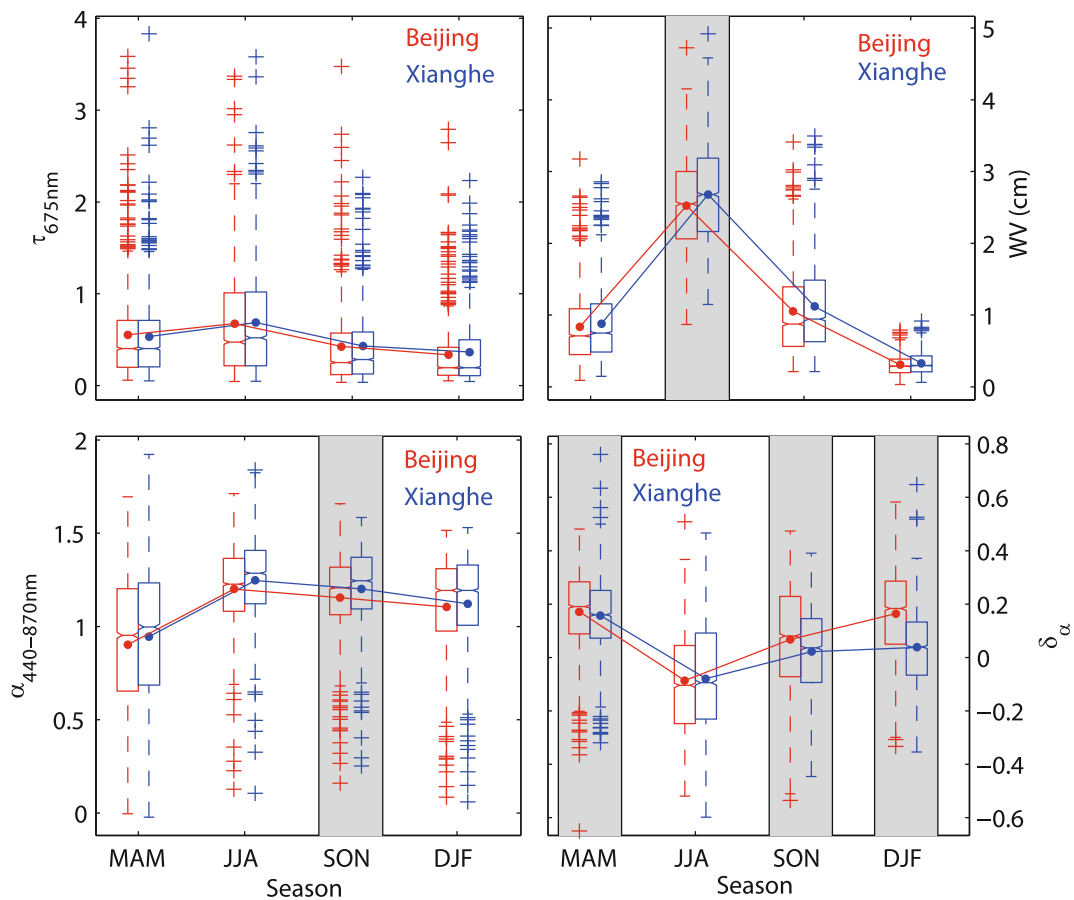


**Fig. 3.** Seasonal statistics and inter-comparison of aerosol optical depth (AOD) ( $\tau_{675\text{nm}}$ ), water vapor content (WV), Ångström exponent (AE) ( $\alpha_{440-870\text{nm}}$ ), and AE difference  $\delta_\alpha$  ( $\alpha_{440-675\text{nm}} - \alpha_{675-870\text{nm}}$ ) at the Beijing and Xianghe sites. The ends of the boxes, the ends of the whiskers, and the short line across each box represent the 25th and 75th percentiles, the 5th and 95th percentiles, and the median, respectively. The mean is represented by the solid circles. The median values are significantly different at the 95% level if they are shaded.

Eck et al., 2010). Larger AODs are observed in spring and summer relative to fall and winter. The minimum AE is observed in spring as a consequence of occasional dust events. Correspondingly, the FMF shown in Fig. 4 reaches a minimum in spring due to the impact of the coarse-mode dust aerosol. The maximum WV is observed in summer, the rainy season when WV is approximately 2–10 times larger than that in other seasons. There are always some samples with AOD larger than the median plus 1.5 times the difference between the 75th and 25th percentiles. This clearly indicates a positively skewed distribution having a “long tail”, which is pulled in the larger-AOD direction. The skewness of the remaining parameters is much less than that of AOD. The minimum  $\delta_\alpha$  ( $< 0$ ) and the maximum FMF in summer indicate the dominance of fine-mode aerosols. It has been pointed out that a combination of increasing AOD and negative  $\delta_\alpha$  indicates hygroscopic and/or coagulation growth from the aging of fine-mode aerosols (Gobbi et al., 2007). The maximum of the effective radius of the fine-mode aerosols in summer shown in Fig. 4 also proves the presence of hygroscopic growth of fine-mode aerosols.

The outstanding feature is that the seasonal medians of

AOD at the two stations are significantly correlated. The correlation coefficients and the absolute differences between AOD at the two stations are larger than 0.84 and less than 0.05, respectively. A good agreement in AOD at these two sites indicates that aerosol pollution in the Greater Beijing area is regional in nature. This feature occurs not only in spring (Eck et al., 2005; Xia et al., 2005), but also in other seasons. This result clearly reveals that the aerosol pollution is regional in nature, which is consistent with the results reported by Xia et al. (2013b). Correlation analysis of AERONET AODs at Beijing and Terra level 2.0 pixel AODs show that a strong correlation ( $R > 0.7$ ) persists for large and strongly anisotropic areas covering 17 000 km<sup>2</sup> in winter to 100 000 km<sup>2</sup> in fall. The zone with larger  $R$  generally extends in a southwesterly direction from the polluted areas to relatively clean areas in the northeast. WV at Xianghe is generally larger than that at Beijing. This is mostly because this station is much closer to the Bohai Sea. AE at Xianghe is also significantly correlated to that at Beijing and the correlation coefficients range from 0.84 in summer to 0.93 in winter. The absolute differences of AE between the two sites are less than 0.05 and the difference is significant only in fall. Al-

though the correlation coefficients of  $\delta_\alpha$  at the two stations are larger than 0.66,  $\delta_\alpha$  at Xianghe is significantly smaller than  $\delta_\alpha$  at Beijing in seasons except summer, ranging from 0.01 (winter) to 0.13 (spring). A significant difference in the median  $\delta_\alpha$  between the two stations indicates that the effective radius of the fine-mode aerosols ( $r_f$ ) is quite different. This is supported by the analysis of  $r_f$  retrieved from diffuse radiance measurements (refer to Fig. 4). A significant difference in  $r_f$  ( $\sim 0.005 \mu\text{m}$ ) between the two stations is observed in all seasons except summer.

Seasonal FMFs at Xianghe are always larger than corresponding values at Beijing, although the difference is significant only in fall. The difference in FMF demonstrates a different mixture of fine and coarse particles between the two sites. AAE is widely employed to describe atmospheric aerosol absorption for certain aerosol types (Yang et al., 2009; Bergstrom et al., 2010; Russell et al., 2010). In general, light absorbing carbon (LAC) has an AAE near 1.0 while organic carbon (OC), or organic matter (OM), and dust have larger AAEs (Russell et al., 2010; Chen and Bond, 2010). The mean AAEs (440–870 nm) are 1.43 and 1.52 at Beijing and Xianghe, respectively, close to the short-term mean AAE (1.47) at Xianghe during March 2005 reported by Yang et al. (2009). Summer median AAEs at the two stations are close to each other; however, the median AAEs at Xianghe in the other seasons are significantly larger than those at Beijing and the difference ranges from 0.09 in winter to 0.21 in fall. The relatively smaller AAE at Beijing indicates either a higher BC fraction or lower OM fraction relative to Xianghe. It has been previously shown that the BC volume percentage is higher in Beijing during winter months compared to that at Xianghe (Koven and Fung, 2006). Seasonal statistics of SSA at 440, 675, 870, and 1020 nm are represented as box-and-whisker plots in Fig. 5. SSA increases from spring to summer and then decreases to winter. The low absorption values in summer are also possibly related to water-soluble aerosol with high RH. Studies have shown that SSA in Beijing increases with increasing RH (Roger et al., 2009; Li et al., 2013). Seasonal SSAs at Xianghe are always larger than their corresponding values at Beijing. The differences at 440 (0.012) and 675 nm (0.017) are significant in fall. The differences in SSA at these two wavelengths in other seasons are not significant. The surface wind speed (see online supplementary material) is lowest in fall, which is not favorable for aerosol mixing. Thus, the local-scale aerosol pollution is dominant in fall and the difference in aerosol absorption properties between the two sites is significant during the fall season.

We can see significant differences in SSA at 870 nm (about 0.02) in seasons except summer. SSA at 1020 nm at Xianghe is significantly larger than that at Beijing in fall and winter. The spectral SSA (see online supplementary material) at Beijing and Xianghe shows its highest value at 675 nm, which is independent of season. Urban-industrial aerosols composed of brown carbon contributed both by vehicular traffic and heavy industry show the less absorption at 675 nm than at infrared wavelength (Bond and Bergstrom, 2006). The decreasing trend of SSA at

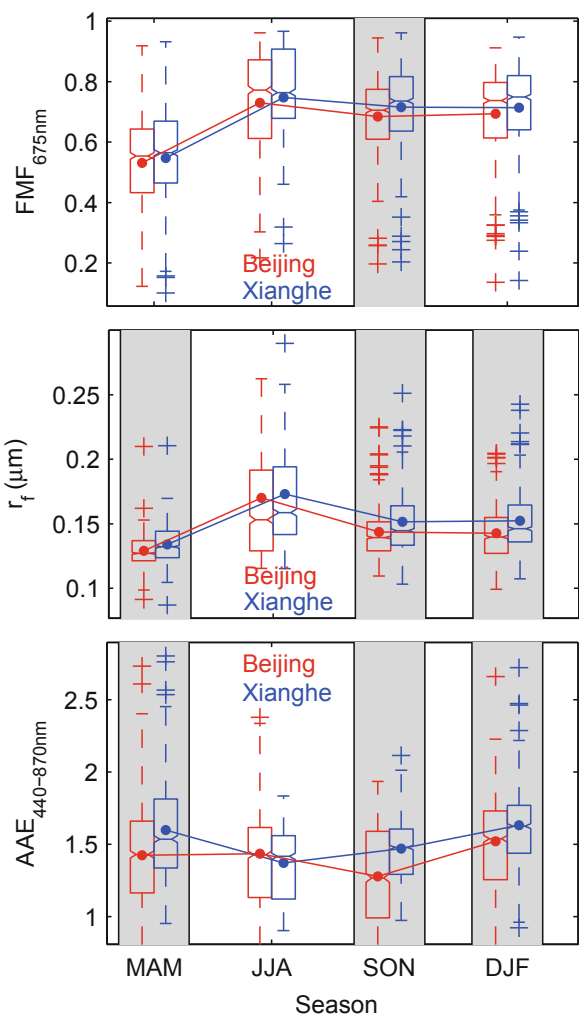


**Fig. 4.** As in Fig. 3, except for fine-mode fraction (FMF) at 675 nm, absorption Ångström exponent (AAE) (440–870 nm), and the fine-mode effective radius ( $r_f$ ).

longer wavelengths is more significant in Beijing compared to Xianghe, such that the absorption difference between the two sites is more significant at longer wavelengths.

Given the fact that refractive index is an important parameter determining SSA, similar analysis is performed for the real and imaginary part of the refractive index in Figs. 6 and 7. The minimum real and imaginary parts of the refractive index in summer are likely associated with high RH and resultant aerosol hygroscopic growth (Dubovik et al., 2002), which is in good accordance with the fact that the maximum fine mode effective radius is observed in this season. There is generally no significant difference in the imaginary part at 440 and 675 nm, although the imaginary part at Xianghe is generally smaller than that at Beijing. At longer wavelengths (870 and 1020 nm), the difference in the imaginary part between the two stations is generally larger than that at shorter wavelengths, and the difference is significant in fall. The real part at wavelengths  $> 440$  nm at Xianghe is significantly smaller than that at Beijing in spring, indicating a relatively smaller scattering ability of aerosols at Xianghe.

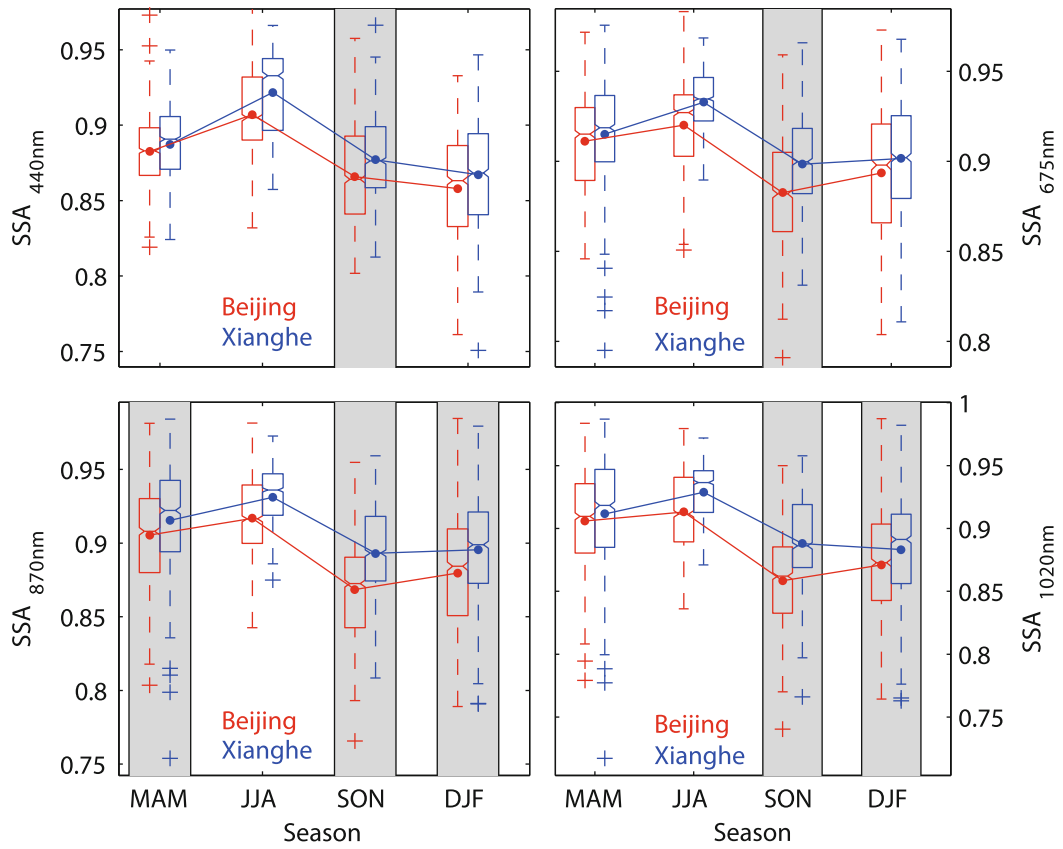


**Fig. 5.** As in Fig. 3, except for the single scattering albedo (SSA) at four wavelengths.

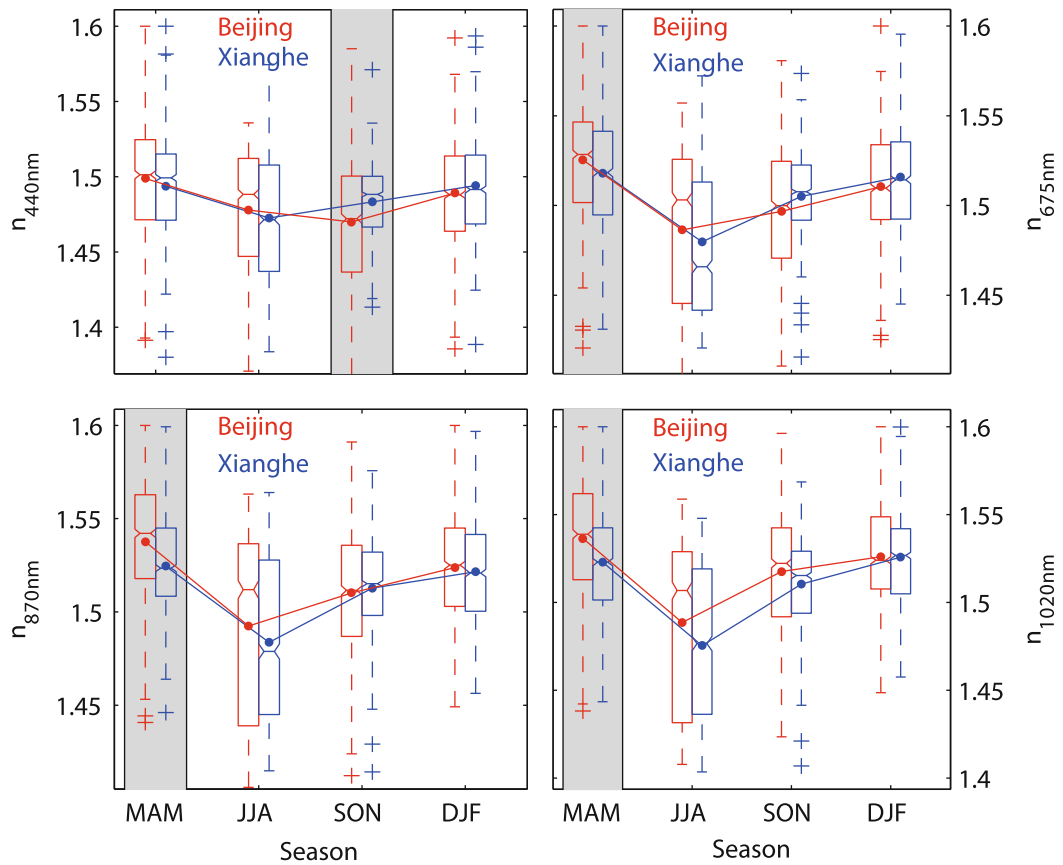


**Fig. 6.** As in Fig. 3, except for the real part of the refractive index.

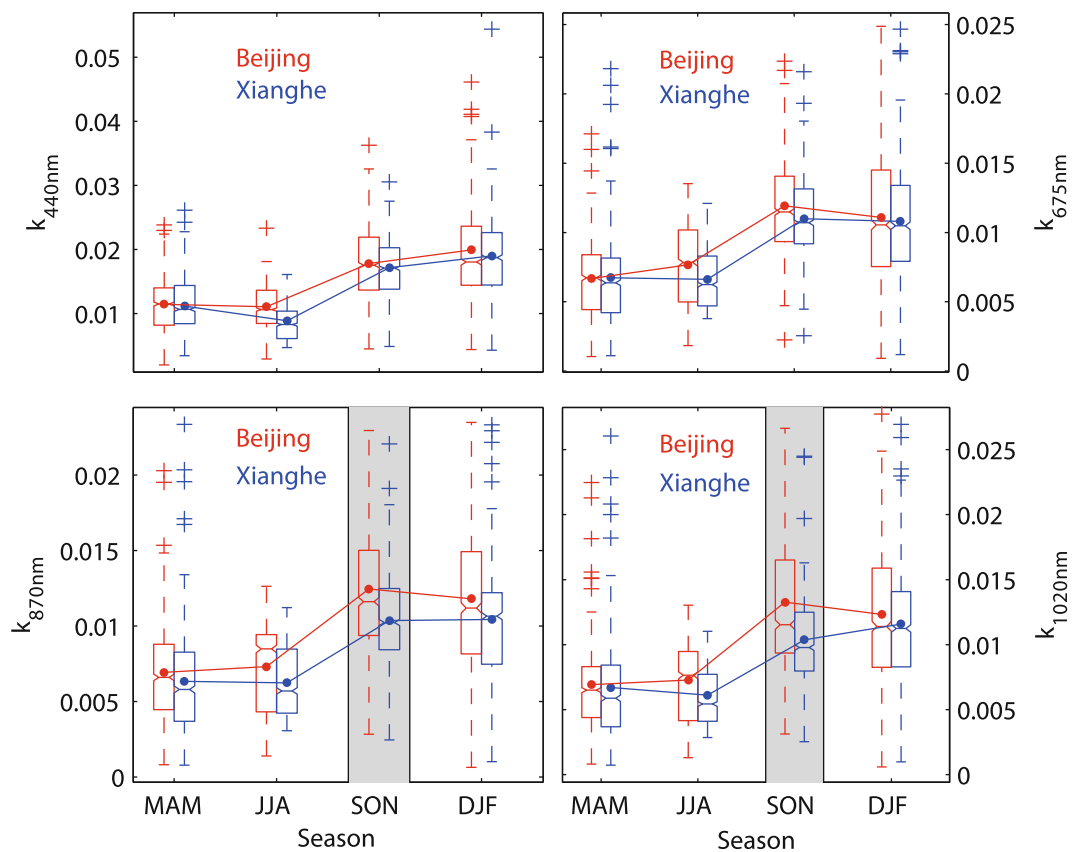


Fig. 7. As in Fig. 3, except for the imaginary part of the refractive index.

## 5. Discussion and conclusions

AERONET aerosol data at Beijing and Xianghe are used to investigate the temporal and spatial distribution of aerosol optical properties on the NCP. The fact that very close values of AOD are observed at the two sites on the NCP (one urban and the other suburban; 70 km apart) implies that aerosol pollution in the Greater Beijing area is regional in nature, which occurs not only in spring, but also in other seasons. Column-integrated aerosol loadings are generally similar, but we also see a significant difference in FMF (675 nm), the real and imaginary parts of the refractive index, and thereby SSA, and the difference is seasonally dependent. This feature is found to be more prominent in fall when FMF, AAE (440–870 nm),  $r_f$ , the imaginary part of the refractive index at 870 and 1020 nm, and SSA at four wavelengths are significantly different at the two stations. Fall is the harvest season on the NCP. Farmers generally burn crop residues for the disposal of agricultural waste. The practice occurs in eastern agricultural regions (Xia et al., 2013b). The significant difference found in aerosol optical and physical properties in fall is likely due to significant emissions of smoke aerosols in fall in rural areas and relatively stable weather in this season (not favorable for mixing). Since open fires are characterized by high  $\text{CO}/\text{NO}_x$  ratios (Wang et al., 2002; Streets et al., 2003), as supported by *in situ* measurements in March 2005 (Li et al., 2007a), simultaneous measurements of  $\text{NO}_x$  and CO are helpful for the characterization of smoke emission sources.

The SSA differences at 440 and 675 nm between the two sites are not significant, but the difference in SSA is significant as wavelength increases, suggesting that coarse-mode aerosol at the Beijing site is more absorptive. A similar conclusion was also drawn by Eck et al. (2010). It could be that the coating of coarse-mode particles by absorbing fine-mode aerosols that contain BC, as observed in ACE-Asia (Asian Pacific Regional Aerosol Characterization Experiment) (Arimoto et al., 2006), results in lower SSA at Beijing. In addition, some coarse-mode particles may not be dust, such as fly ash from coal combustion and/or emissions from briquette fuel made of coal dust and silt mixtures on the NCP (Yang et al., 2009; Eck et al., 2010), resulting in the lower SSA at Beijing.

Beijing shows higher absorption than Xianghe for the 440 through 1020 nm wavelengths, although the difference is not significant in some cases. Significant differences in AAE and  $r_f$  indicate that there are differences in aerosol physical and chemical properties between urban and suburban regions on the NCP. It is therefore necessary for long-term observations of chemical properties to be used in future work to investigate and confirm the aerosol absorption difference between the two sites. Detailed comparison of aerosol optical, physical and chemical properties requires further study.

**Acknowledgements.** This work was supported by the National Basic Research Program of China (Grant Nos. 2010CB950804 and



2013CB955801), National Natural Science Foundation of China (Grant No. 41475027) and the Chinese Strategic Priority Research Program—Climate Change: Carbon Budget and Relevant Issues (Grant No. XDA05040202).

## REFERENCES

- Arimoto, R., and Coauthors, 2006: Characterization of Asian dust during ACE-Asia. *Global Planet Change*, **52**(1–4), 23–56.
- Bergstrom, R. W., P. Pilewskie, P. B. Russell, J. Redemann, T. C. Bond, P. K. Quinn, and B. Sierau, 2007: Spectral absorption properties of atmospheric aerosols. *Atmos. Chem. Phys.*, **7**(23), 5937–5943.
- Bergstrom, R. W., K. S. Schmidt, O. Coddington, P. Pilewskie, H. Guan, J. M. Livingston, J. Redemann, and P. B. Russell, 2010: Aerosol spectral absorption in the Mexico City area: Results from airborne measurements during MILAGRO/INTEX B. *Atmos. Chem. Phys.*, **10**(13), 6333–6343.
- Bond, T. C., and R. W. Bergstrom, 2006: Light absorption by carbonaceous particles: An investigative review. *Aerosol Science and Technology*, **40**(1), 27–67.
- Che, H. Z., and Coauthors, 2009: Instrument calibration and aerosol optical depth validation of the China Aerosol Remote Sensing Network. *J. Geophys. Res.*, **114**, doi: 10.1029/2008jd011030.
- Chen, Y., and T. C. Bond, 2010: Light absorption by organic carbon from wood combustion. *Atmos. Chem. Phys.*, **10**(4), 1773–1787.
- Dubovik, O., and M. D. King, 2000: A flexible inversion algorithm for retrieval of aerosol optical properties from Sun and sky radiance measurements. *J. Geophys. Res.*, **105**(D16), 20 673–20 696.
- Dubovik, O., B. N. Holben, T. F. Eck, A. Smirnov, Y. J. Kaufman, M. D. King, D. Tanre, and I. Slutsker, 2002: Variability of absorption and optical properties of key aerosol types observed in worldwide locations. *J. Atmos. Sci.*, **59**(3), 590–608.
- Dubovik, O., and Coauthors, 2006: Application of spheroid models to account for aerosol particle nonsphericity in remote sensing of desert dust. *J. Geophys. Res.*, **111**(D11), doi: 10.1029/2005jd006619.
- Eck, T. F., and Coauthors, 2005: Columnar aerosol optical properties at AERONET sites in central eastern Asia and aerosol transport to the tropical mid-Pacific. *J. Geophys. Res.*, **110**(D6), doi: 10.1029/2004jd005274.
- Eck, T. F., and Coauthors, 2008: Spatial and temporal variability of column-integrated aerosol optical properties in the southern Arabian Gulf and United Arab Emirates in summer. *J. Geophys. Res.*, **113**(D1), doi: 10.1029/2007jd008944.
- Eck, T. F., and Coauthors, 2010: Climatological aspects of the optical properties of fine/coarse mode aerosol mixtures. *J. Geophys. Res.*, **115**, doi: 10.1029/2010jd014002.
- Fan, X. H., P. Goloub, J. L. Deuzé, H. B. Chen, W. X. Zhang, D. Tanré, and Z. Q. Li, 2008: Evaluation of PARASOL aerosol retrieval over North East Asia. *Remote Sens. Environ.*, **112**(3), 697–707.
- Fan, X. H., H. B. Chen, L. F. Lin, Z. G. Han, and P. Goloub, 2009: Retrieval of aerosol optical properties over the Beijing area using POLDER/PARASOL satellite polarization measurements. *Adv. Atmos. Sci.*, **26**(6), 1099–1107, doi: 10.1007/s00376-009-8103-x.
- Fan, X. H., H. B. Chen, and X. A. Xia, 2013: Progress in observation studies of atmospheric aerosol radiative properties in China. *Chinese J. Atmos. Sci.*, **37**(2), 477–498. (in Chinese)
- Garland, R. M., and Coauthors, 2009: Aerosol optical properties observed during Campaign of Air Quality Research in Beijing 2006 (CAREBeijing-2006): Characteristic differences between the inflow and outflow of Beijing city air. *J. Geophys. Res.*, **114**, doi: 10.1029/2008jd010780.
- Gobbi, G. P., Y. J. Kaufman, I. Koren, and T. F. Eck, 2007: Classification of aerosol properties derived from AERONET direct sun data. *Atmos. Chem. Phys.*, **7**, 453–458.
- Guo, J. P., Y. Xue, C. X. Cao, H. Zhang, J. Guang, X. Y. Zhang, and X. W. Li, 2009: A synergic algorithm for retrieval of aerosol optical depth over land. *Adv. Atmos. Sci.*, **26**(5), 973–983, doi:10.1007/s00376-009-7218-4.
- Hao, J. M., and L. T. Wang, 2005: Improving urban air quality in China: Beijing case study. *J. Air. Waste Manag. Assoc.*, **55**(9), 1298–1305.
- Holben, B. N., and Coauthors, 2001: An emerging ground-based aerosol climatology: Aerosol optical depth from AERONET. *J. Geophys. Res.*, **106**(D11), 12 067–12 097.
- Koven, C. D., and I. Fung, 2006: Inferring dust composition from wavelength-dependent absorption in Aerosol Robotic Network (AERONET) data. *J. Geophys. Res.*, **111**(D14), doi: 10.1029/2005jd006678.
- Li, C., and Coauthors, 2007a: In situ measurements of trace gases and aerosol optical properties at a rural site in northern China during East Asian study of tropospheric aerosols: An international regional experiment 2005. *J. Geophys. Res.*, **112**(D22), doi: 10.1029/2006jd007592.
- Li, Z., and Coauthors, 2013: Aerosol physical and chemical properties retrieved from ground-based remote sensing measurements during heavy haze days in Beijing winter. *Atmos. Chem. Phys.*, **13**(20), 10 171–10 183.
- Li, Z. Q., F. Niu, K. H. Lee, J. Y. Xin, W. M. Hao, B. Nordgren, Y. S. Wang, and P. C. Wang, 2007b: Validation and understanding of moderate resolution imaging spectroradiometer aerosol products (C5) using ground-based measurements from the handheld Sun photometer network in China. *J. Geophys. Res.*, **112**(D22), doi: 10.1029/2007jd008479.
- Li, Z. Q., and Coauthors, 2007c: Aerosol optical properties and their radiative effects in northern China. *J. Geophys. Res.*, **112**(D22), doi: 10.1029/2006jd007382.
- Li, Z. Q., and Coauthors, 2011: East Asian Studies of Tropospheric Aerosols and their Impact on Regional Climate (EAST-AIRC): An overview. *J. Geophys. Res.*, **116**, doi: 10.1029/2010jd015257.
- Li, Z. Q., and Coauthors, 2014: Observations of residual submicron fine aerosol particles related to cloud and fog processing during a major pollution event in Beijing. *Atmospheric Environment*, **86**, 187–192.
- Lin, J. T., D. Pan, and R. X. Zhang, 2013: Trend and interannual variability of Chinese air pollution since 2000 in association with socioeconomic development: A brief overview. *Atmos. Ocean Sci. Lett.*, **6**, 84–89.
- Luo, Y. F., D. R. Lu, X. J. Zhou, W. L. Li, and Q. He, 2001: Characteristics of the spatial distribution and yearly variation of aerosol optical depth over China in last 30 years. *J. Geophys. Res.*, **106**(D13), 14 501–14 513.
- Lyapustin, A., and Coauthors, 2011: Reduction of aerosol absorption in Beijing since 2007 from MODIS and AERONET. *Geophys. Res. Lett.*, **38**(10), doi: 10.1029/2011gl047306.
- Mi, W., Z. Q. Li, X. G. Xia, B. Holben, R. Levy, F. S. Zhao, H.

- B. Chen, and M. Cribb, 2007: Evaluation of the moderate resolution Imaging spectroradiometer aerosol products at two aerosol robotic network stations in china. *J. Geophys. Res.*, **112**(D22), doi: 10.1029/2007jd008474.
- Nishizawa, T., N. Sugimoto, I. Matsui, A. Shimizu, X. G. Liu, Y. H. Zhang, R. H. Li, and J. Liu, 2010: Vertical distribution of water-soluble, sea salt, and dust aerosols in the planetary boundary layer estimated from two-wavelength backscatter and one-wavelength polarization lidar measurements in Guangzhou and Beijing, China. *Atmospheric Research*, **96**(4), 602–611.
- Qiu, J. H., and L. Q. Yang, 2000: Variation characteristics of atmospheric aerosol optical depths and visibility in North China during 1980–1994. *Atmos. Environ.*, **34**(4), 603–609.
- Roger, J. C., B. Guinot, H. Cachier, M. Mallet, O. Dubovik, and T. Yu, 2009: Aerosol complexity in megacities: From size-resolved chemical composition to optical properties of the Beijing atmospheric particles. *Geophys. Res. Lett.*, **36**, doi: 10.1029/2009gl039238.
- Russell, P. B., and Coauthors, 2010: Absorption Angstrom Exponent in AERONET and related data as an indicator of aerosol composition. *Atmos. Chem. Phys.*, **10**(3), 1155–1169.
- Streets, D. G., and Coauthors, 2003: An inventory of gaseous and primary aerosol emissions in Asia in the year 2000. *J. Geophys. Res.*, **108**(D21), doi: 10.1029/2002jd003093.
- Wang, T., T. F. Cheung, Y. S. Li, X. M. Yu, and D. R. Blake, 2002: Emission characteristics of CO, NO<sub>x</sub>, SO<sub>2</sub> and indications of biomass burning observed at a rural site in eastern China. *J. Geophys. Res.*, **107**(D12), doi: 10.1029/2001jd000724.
- Wang, S. X., and Coauthors, 2010: Quantifying the air pollutants emission reduction during the 2008 Olympic Games in Beijing. *Environmental Science & Technology*, **44**(7), 2490–2496.
- Wang, W. T., T. Primbs, S. Tao, and S. L. M. Simonich, 2009: Atmospheric particulate matter pollution during the 2008 Beijing Olympics. *Environmental Science & Technology*, **43**(14), 5314–5320.
- Wild, C., and G. Seber, 1999: *Chance Encounters: A First Course in Data Analysis and Inference*. 1st ed., Wiley, 632 pp.
- Xia, X. A., H. B. Chen, P. C. Wang, X. M. Zong, J. H. Qiu, and P. Goloub, 2005: Aerosol properties and their spatial and temporal variations over North China in spring 2001. *Tellus B*, **57**(1), 28–39.
- Xia, X. A., H. B. Chen, P. C. Wang, W. X. Zhang, P. Goloub, B. Chatenet, T. F. Eck, and B. N. Holben, 2006: Variation of column-integrated aerosol properties in a Chinese urban region. *J. Geophys. Res.*, **111**(D5), 10.1029/2005jd006203.
- Xia, X., H. Chen, P. Goloub, W. Zhang, B. Chatenet, and P. Wang, 2007: A compilation of aerosol optical properties and calculation of direct radiative forcing over an urban region in northern China. *J. Geophys. Res.*, **112**(D12), doi: 10.1029/2006jd008119.
- Xia, X. A., H. B. Chen, P. Goloub, X. M. Zong, W. X. Zhang, and P. C. Wang, 2013a: Climatological aspects of aerosol optical properties in North China Plain based on ground and satellite remote-sensing data. *J. Quant. Spectrosc. Ra.*, **127**, 12–23.
- Xia, X. A., X. M. Zong, and L. Sun, 2013b: Exceptionally active agricultural fire season in mid-eastern China in June 2012 and its impact on the atmospheric environment. *J. Geophys. Res.*, **118**, doi: 10.1002/jgrd.50770.
- Yang, M., S. G. Howell, J. Zhuang, and B. J. Huebert, 2009: Attribution of aerosol light absorption to black carbon, brown carbon, and dust in China—Interpretations of atmospheric measurements during EAST-AIRE. *Atmos. Chem. Phys.*, **9**(6), 2035–2050.
- Yu, X. N., T. T. Cheng, J. M. Chen, and Y. Liu, 2007: Climatology of aerosol radiative properties in northern China. *Atmospheric Research*, **84**(2), 132–141.
- Zhang, R., and Coauthors, 2013: Chemical characterization and source apportionment of PM<sub>2.5</sub> in Beijing: Seasonal perspective. *Atmos. Chem. Phys.*, **13**(14), 7053–7074.